Eur. Phys. J. E **8**, 167–173 (2002)
DOI 10.1140/epje/i2001-10090-x

THE EUROPEAN PHYSICAL JOURNAL E
EDP Sciences

Confinement-induced differences between dielectric normal modes and segmental modes of an ion-conducting polymer

K. Kojio, S. Jeon, and S. Granick[a]

Department of Materials Science & Engineering, University of Illinois at Urbana-Champaign, Urbana, IL 61801, USA

Received 31 August 2001 and Received in final form 30 October 2001

Abstract. Dielectric measurement in the range 0.1 Hz to 1 MHz were used to study the motions of polymers and ions in an ion-conducting polymer, polypropylene oxide containing small quantities (on the order of 1%) of lithium ions ($LiClO_4$), confined as a sandwich of uniform thickness between parallel insulating mica surfaces. In the dielectric loss spectrum, we observed three peaks; they originated from the normal mode of the polymer, segmental mode of the polymer, and ion motions. With decreasing film thickness, the peak frequencies corresponding to the normal mode and ion motion shifted to lower frequencies, indicating retardation due to confinement above 30 nm. This was accompanied by diminished intensity of the dielectric normal-mode relaxation, suggesting that confinement diminished the fluctuations of the end-to-end vector of the chain dipole in the direction between the confining surfaces. On the contrary, the segmental mode was not affected at that thickness. Finally, significant retardation of the segmental mode was observed only for the thinnest film (14 nm). The different dynamical modes of the polymer (segmental and slowest normal modes) respond with different thickness and temperature dependence to confinement.

PACS. 82.35.Gh Polymers on surfaces; adhesion – 61.25.Hq Macromolecular and polymer solutions; polymer melts; swelling

1 Introduction

The classic, long-standing problem of the glass transition [1–3] has been revitalized by the idea that some kind of cooperativity length enters naturally into the statement of this problem [4–9]. This has motivated a great deal of experimental work to study shifts of the glass transition when a glass-forming liquid is confined in one or more directions [10–12]. In this study, we focus for what we believe to be the first time on an ion-conducting polymer.

Several issues render the problem of T_g more problematical in a confined geometry than in bulk systems. Specific boundary effects (a curved pore-space or a parallel geometry; attractive or repulsive surface; "hard" solid boundary or "soft" boundary comprised of air or vacuum) are one difficulty. In these systems where a large portion of the sample is necessarily in intimate contact with its boundary, it is not evident that a universal answer (independent of the specific boundary) should be expected. Indeed, different measures of T_g sometimes do not agree when it comes to specifying the point of glass transition in these anisotropic thin films. These methods include, for example, thermal expansivity, translational diffusion, and segmental mobility measured by dielectric or rheological methods [12]. But in bulk systems, these methods do agree.

A third problematical point is the limited availability of suitable experimental systems. This is a particular problem when one seeks to eliminate strong attraction of a sample to its boundary. It is true that the study of free-standing polymer films, thin strips positioned in an environment of air or vacuum, has presented a refreshing simplification, leading to major advances [13,14], but their study is limited to situations in which the films cannot, owing to high viscosity, bead up to minimize their surface area. This limits their study to temperatures below the glass transition temperature. The present study, in contrast, focuses on behavior at temperatures above T_g. Confinement between partially wetting solid surfaces can be used to study kinetically stable films in which strong surface attraction is avoided [15,16].

Turning specifically to the problem of ion-conducting polymers, we note that it is well known that polyethers such as polyethylene oxide, polypropylene oxide, and polytetramethylene oxide show high DC conductivity after addition of alkali metal ions. The polyether dissolves alkali metal salts and it is reasonable to suppose that its dissociated alkali metal ions are tetrahedrally coordinated by polyether oxygen. Although the conduction mechanism is unclear, it is generally accepted that the dissociated metal cations contribute to DC conductivity by achieving mobility through the micro-Brownian motion of polymer segments [17,18]. Conversely, the dissociated

[a] e-mail: sgranick@uiuc.edu

anions move independently of the polymer motion [19]. These ion-conductive polymers have been studied extensively mainly because of their importance in industrial applications such as a polymer battery. That is why most studies to date have focused on the motion of ions [20–25], not on the motion of the polymer within which the ions are embedded.

Among the polyethers, polypropylene oxide (PPO) has some interesting features. It is an amorphous flexible polymer that possess a strong dipole along the chain dipole and another significant component perpendicular to it. Therefore it displays characteristic relaxation peaks in both directions when an electric field is applied [26]. The backbone relaxation, so-called normal-mode relaxation, is usually hidden by segmental-mode relaxation especially if the molecular weight is less than 1000 g mol^{-1}. Also, the glass transition temperature of polypropylene oxide is unusually insensitive to molecular weight; it shows no dependence on molecular weight down to 400 g mol^{-1} [26]. This absence of free ends effect is attributed to the hydrogen bonding which reduces the mobility of free ends. This hydrogen bonding effect was confirmed by replacing oxygen with sulfur, which is incapable of hydrogen bonding [27]. Unlike polypropylene oxide, polypropylene sulfide shows the expected significant decrease of glass transition temperature for lower mass.

These interesting properties of polypropylene glycol led to previous studies of its dynamics not only in the bulk but also in confined states [28]. However, we are not aware of any previous study of confinement effects on the normal-mode relaxation; previous concern has been with segmental motions. Most previous experiments have used porous materials to confine the pure liquid [29,30]. In this case, samples were usually low-molecular-weight liquids because it is so difficult to impregnate high-molecular-weight polymers into a porous substrate.

Recently, our group introduced methods to study the dielectric response of thin films confined between atomically smooth surfaces of mica [15,16]. The enabling idea was to employ spin casting to produce thin films on atomically smooth mica sheets whose backside was coated with silver so that surface separation could be determined using multiple beam interferometry. This method has many advantages. First of all, the geometry is flat and there is no ambiguity about the geometry, unlike the case of porous substrates in which porosity and pore filling are nonuniform. Secondly, spin casting is a very efficient way to produce a thin film of high-molecular-weight polymer. Third, film thickness can be very accurately measured, ±0.2–0.5 nm, by multiple-beam interferometry. Finally, mica surface can be easily modified chemically to study the effects of changing the surface chemistry.

Here, we used broadband dielectric relaxation spectroscopy to study the influence of film thickness on the dielectric relaxation of polypropylene oxide thin films, confined in sandwich geometry, and containing small amounts of $LiClO_4$. The confining surfaces conditions, freshly cleaved muscovite mica, comprised partially wetting solids between which kinetically stable films could be produced, although dewetting cannot be eliminated completely. The main results are as follows. First, both ion relaxation and normal-mode relaxation showed retardation when they were confined, and this effect was observed, in films as thick as 0.1 μm, starting at $\sim$ 100 K above T_g. Second, local segmental dynamics appeared to be unaffected down to 30 nm thickness. However, as the film thickness decreased further, segmental dynamics were also retarded and the glass transition temperature increased.

2 Experimental

2.1 Sample and methods

The PPO samples were purchased from Aldrich with molecular weights $M_n = 3,500$ g mol^{-1}. Unfortunately, the supplier had not characterized the molecular weight distribution and methods to do so were not available in our laboratory. Samples of lesser molecular weight were not studied because dewetting was too rapid (see the discussion below). Samples of larger molecular weight (had they been available) would have been unattractive because of the need to capture both the normal-mode and segmental-mode dielectric relaxation peaks within the same window of frequency. For the sample studied in this paper, the glass transition temperature was around 200 K.

The PPO and $LiClO_4$ (Aldrich) were dissolved in methanol, then mixed together. The concentration of $LiClO_4$ was 1% (one Li^+ ion per 100 PPO segmental units). After complete dissolution, this mixture was kept in a vacuum oven at 333 K for 6 h in order to remove the solvent. In working with atomically smooth mica, film thickness was defined with precision. Sufficiently thin mica allowed Ag electrodes to be sputter-deposited onto the backside, using methods standard in the surface forces apparatus technique [15], enabling the sample thickness to be measured by multiple-beam interferometry, while at the same time enabling dielectric response to be measured over a broad range of frequency.

The samples were prepared by spin-coating onto one mica sheet (from methanol 0.1 to 2 wt.% depending on the desired film thickness). Capillary forces pulled a second mica sheet onto the underlying spin-coated sample, creating a sandwich geometry.

A detailed description of the experimental technique was reported previously [16]. The measurements employed a Solartron 1260 Gain-Phase Impedance Analyzer connected to a Solartron 1296 Dielectric Interface.

The temperature uniformity at the sample was ±0.1 K. Briefly, temperature was controlled over a wide range by placing the sample within an insulated chamber contained within a Dewar flask through which there passed gas from evaporation of liquid nitrogen that had been preheated as needed. The fractional change of thickness between our lowest measurement temperatures and room temperature (the preparation temperature), owing to thermal expansion, was approximately 4.5%. The range of measurement temperatures that we report below was dictated by the need to keep dispersions within the available frequency

range: > 1 Hz to avoid distortion from polar surface impurities and <∼ 3 MHz by instrumental limitations.

Dielectric measurements were usually made in the order of descending temperature but control experiments verified reversibility when the temperature was raised to 293 K and then lowered back to 210 K for repeat measurement. About 10 min were required for measurements after about 30 min to equilibrate at each temperature. Thickness measured by multiple-beam interferometry would usually show uniform thickness over a spot size of 1 cm.

2.2 Analysis of dielectric measurements

Elsewhere it was discussed that when the response to sinusoidal input electric field at frequency f is decomposed into one component in-phase with the field, and a second component in-phase with its rate of change, the former (real) component is dominated by the mica buffer sheets between the electrodes and sample, and the latter (loss) component, $C''(f)$, contains an immeasurably small contribution from the mica sheets and reflects only the PI sample [15]. Specifically, for the measurement of polymer sample between two parallel sheets of mica the complex capacity C^* is given as

$$C^* = \left[\frac{1}{C_\mathrm{m}} + \frac{1}{C^*_\mathrm{PI}}\right]^{-1} = C_\mathrm{m}\left[1 + \frac{t_\mathrm{PI}\varepsilon_\mathrm{m}}{t_\mathrm{m}\varepsilon^*_\mathrm{PI}}\right]^{-1}, \qquad (1)$$

where C^*_PI is complex capacitance of the polymer interface, C_m is the capacitance of the two mica layers, t_m is the total thickness of the two mica layers, and ε_m is the (ω-insensitive) dielectric constant of mica, and t_PI is the thickness of the thin, spin-coated PI layer. For this setup, C_m is identical to the capacity measured for the bare mica-mica contact, and t_m and t_PI are known from optical interferometry. The quantity ε_m can be calculated from C_m (if the electrode area is known), or can be replaced by a literature value. Thus, in principle it is possible to evaluate $\varepsilon_\mathrm{PI}{}^*$ from experimentally measured values, but the method requires accurate calibration of the empty cell (bare mica capacitance).

In our current experimental setup it was not possible to perform these experiments in an atmosphere sufficiently dry to obtain a sufficiently reliable evaluation of C_m (mica-mica contact). The influence of moisture condensed on the mica surfaces became plain when measurements were performed in nominal mica-mica contact (two cleaved mica sheets placed in contact). The ratio C''/C' was variable between experiments, as discussed elsewhere [15]. There then resulted a large uncertainty in the capacitance of the two mica layers, C_m, and it was not possible to be confident that C_m measured for mica-mica contact remained the same after spin-coating with PI. Therefore in the results that follow, the raw data $C''(f)$ will be presented. Because the out-of-phase contribution of the sample cell (mica) to $C''(f)$ was negligible, its frequency dependence is believed to have been the same as for the polyisoprene sample of interest.

3 Results

3.1 Reliability of measurements

Although it is an interesting question to consider by what mechanism the films were able to dewet when confined between the two rather rigid solid boundaries of mica, in practice they often did. Dewetting was easily visible in an optical microscope. Our attempts failed to perform analogous experiments with the same PPO sample but without added $LiClO_4$. We attribute our greater success ratio with $LiClO_4$ added to the higher viscosity of those samples. Enhanced viscosity is known to inhibit dewetting [31]. In attempts to study dependence on molecular weight we also investigated other samples, but in those samples the dewetting problem was even more severe. Therefore this study is confined to a single sample, of the largest available molecular weight.

Spot control experiments verified reversibility when the samples were quenched to a low temperature soon after spin-coating. After dielectric measurements were made at low temperature, the temperature was raised to 25 °C and then lowered back to −40 °C for repeat measurement. Because of reversibility, because measurements in the range −40 to 0 °C were stable (time independent over a period of hours), and because of quantitative reproducibility between independent experiments with different time and temperature histories, it was concluded that dewetting processes did not contribute to the results described below.

3.2 Identification of relaxation modes

The PPO molecule has dipole moments both parallel and perpendicular to the chain direction. The parallel component contributes to the dielectric relaxation through an overall motion of chain molecules, because its vector sum is proportional to the end-to-end distance of each chain. On the contrary, the perpendicular component contributes through the local fluctuation of individual segmental units. To obtain the characteristic peak positions of PPO used in this study, dielectric measurement were performed. The peaks corresponding to normal and segmental modes were observed with peaks at around 25 Hz and 25000 Hz at 228.0 K, respectively.

It would have been ideal to be able to analyze the raw data for these peaks according to the Havriliak-Negami equation, classical in the study of glasses, but this contains 4 parameters. Robust fits were possible for bulk samples but for the samples of limited thickness, the limited signal to noise precluded robust fits. Therefore the data were fit to simpler Gaussian expressions, to which it was possible to make robust comparison.

Figure 1 shows the frequency dependence of the imaginary part of the capacitance for the PPO-$LiClO_4$ composite measured at 231.2 K as a sample of bulk thickness. The out-of-phase capacitance is plotted against frequency on log-log scales. It can be resolved into three peaks as shown in Figure 1, and we assign these peaks

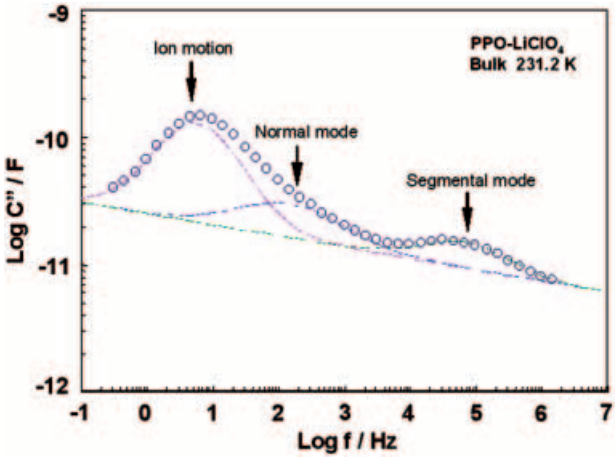

Fig. 1. For a bulk sample, the out-of-phase capacitance is plotted against applied frequency on log-log scales for PPO containing 1% $LiClO_4$ at 231.2 K. This concentration of $LiClO_4$ corresponds approximately to one lithium ion per polymer repeat unit. The peaks at low and high frequency are assigned to ion motion and to segmental motion of the polymer, respectively. Curve-fitting with Gaussian fits (dotted lines) identified the middle peak, which we ascribe to normal-mode relaxation of the polymer.

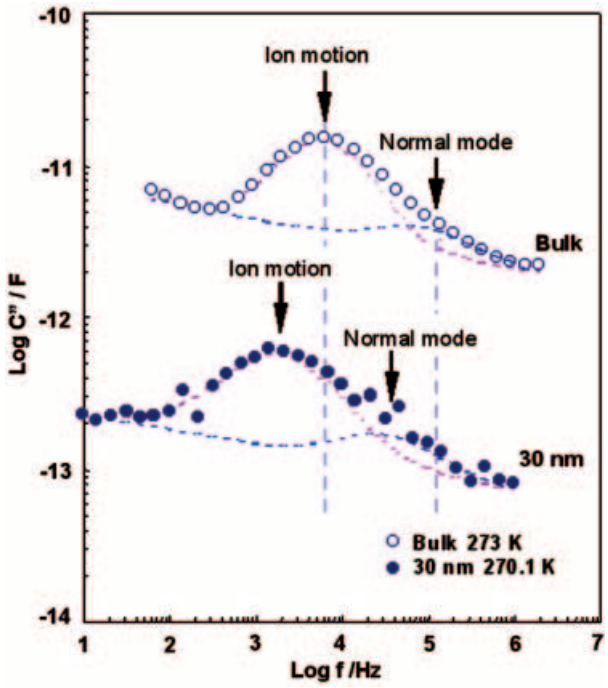

Fig. 2. Illustration of dependence on film thickness. The out-of-phase capacitance is plotted against applied frequency on log-log scales for PPO containing 1% $LiClO_4$ as concerns a sample of bulk thickness (○) and 30 nm thickness (●) measured at 270.3 K and 273.0 K, respectively. The ion peaks and inferred normal-mode peaks (indicated by dotted lines from Gaussian fits to the data) are shown by dotted lines.

to the ion mode, normal mode and segmental mode of PPO. The intensity of the peak observed at lowest frequency increased with increasing salt concentration. This shows clearly that this peak can be assigned to ion motion. Considering the remaining peaks, it is obvious that the segmental peak should fall at higher frequency than the normal-mode peak, and therefore that the normal-mode peak must fall in the middle of the data in Figure 1. On this basis the three peaks, identified in Figure 1, were assigned. The normal-mode peak was inferred by curve-fitting. Note that in the samples whose thickness was limited by confinement between mica sheets, the relative dielectric strengths were not meaningful because the thickness of these spacer layers (on the order of 2-5 μm) was not standardized.

Figure 2 shows the frequency dependence of capacitance of the PPO-$LiClO_4$ composite as concerns a sample of bulk thickness and a sample of thickness 30 nm, measured at 273.0 K and 270.1 K, respectively. The out-of-phase capacitance is plotted against frequency on log-log scales. Two peaks are observed here and they were fitted with multiple Gaussian functions. As in Figure 1, the ion mode relaxation appears at lower frequency than normal-mode relaxation. In the thin film, both the ion mode and the normal mode appear at lower frequency than for the bulk sample.

3.3 Intensity of the relaxation peaks

It is well known that the intensity of normal-mode dielectric relaxation in chains whose dipole lies preferentially along the chain backbone is proportional to the square of the end-to-end distance, but also that the segmental relaxation mode is independent of the end-to-end distance. In PPO without added salt, the dielectric strength of the segmental mode is larger than for the normal mode, but this tendency changes when salt is added. The ratio of normal-mode to segmental-mode peak intensity is a useful approach to deduce polymer conformations in the thin films.

The data for thin films, relative to bulk samples, showed considerable reduction of the normal-mode fluctuations relative to the segmental mode. Extensive quantitative analysis cannot be made at this time because the limited signal to noise in thin-film samples precluded studying the temperature dependence. The temperature-averaged results were as follows. For bulk samples, the intensity of the normal-mode peak dominated; the ratio to the segmental-mode peak was ≈ 1.35 at 240 K. For the thin-film samples the relative intensity was reversed. For thickness 100 nm the ratio was 0.7. For thickness 30 nm it was 0.5.

The suggestive implication is that fluctuations of the end-to-end vector, in the direction normal to the confining surfaces, were considerably less in the thin-film samples than in the bulk. The statement is tentative because we cannot, at present, exclude the possibility that salt concentration in the thin-film samples was enhanced during the spin-coating process, although we have no direct reason to expect this to have been the case. More work is

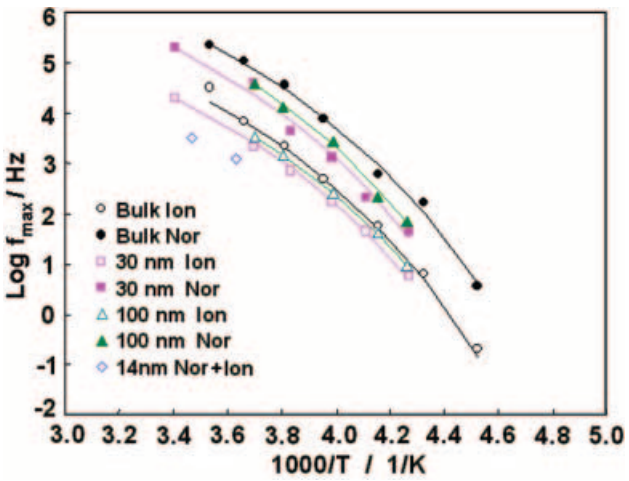

Fig. 3. The peak frequency of the relaxation modes of ion motion (○ bulk, △ 100 nm, □ 30 nm thickness) and normal-mode motion (● bulk, ▲ 100 nm, ■ 30 nm thickness), inferred from data of the kind illustrated in Figure 2, are plotted against inverse absolute temperature. ◇, 14 nm thickness, refer to the combined normal-mode and ion peak. Volger-Fulcher fits were made to this data, as indicated by the solid lines.

needed to test this difficulty of interpretation, and also to quantify this data as a function of temperature.

3.4 Temperature dependence of relaxation peaks

Figure 3 shows the dependence on film thickness and temperature of the fitted peak frequencies of normal-mode and ion mode relaxation for these PPO-$LiClO_4$ composites for a) bulk samples, b) films 100 nm thick, c) films 30 nm thick, and d) films 14 nm thick. The most interesting point here is that these peak frequencies evidently shifted to lower frequency as the film thickness decreased. However, the signal to noise at 14 nm thickness was too low to separate the peaks of normal mode and ion motion by curve fitting, so the peak frequency of their combined relaxation mode was analyzed.

Figure 4 plots the peak frequencies of the segmental-mode relaxation, logarithmically against inverse absolute temperature. It is obvious that the temperature dependence of segmental relaxation was unaffected by confinement for thickness $\geqslant$ 30 nm. But, surprisingly, retardation was observed for the film thickness of 14 nm.

3.5 Confinement-induced shifts

In Figure 3, one sees that at a given temperature, the peak frequency in the thin films was lower than for the bulk samples, and that the discrepancy was larger, the lower the temperature, though even the lowest temperatures examined were considerably above the glass transition temperature. However, retardation of segmental mode was not observed except at the smallest thickness, 14 nm. The insensitivity of the segmental mode to film thickness, but larger dependence of the normal mode to film

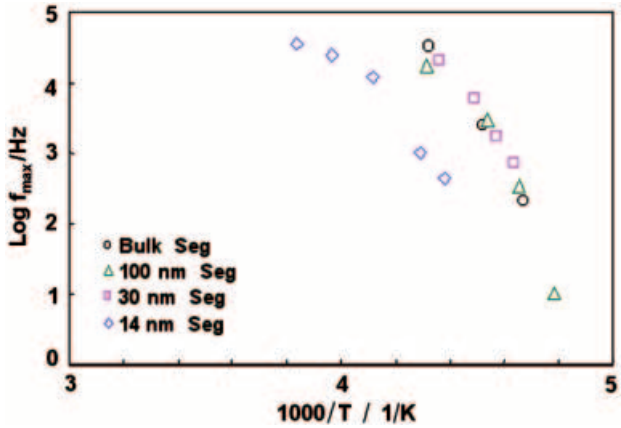

Fig. 4. The peak frequency of the segmental mode (○ bulk, △ 100 nm, □ 30 nm, ◇ 14 nm thick), inferred from data of the kind illustrated in Figure 1, is plotted against inverse absolute temperature at various film thicknesses.

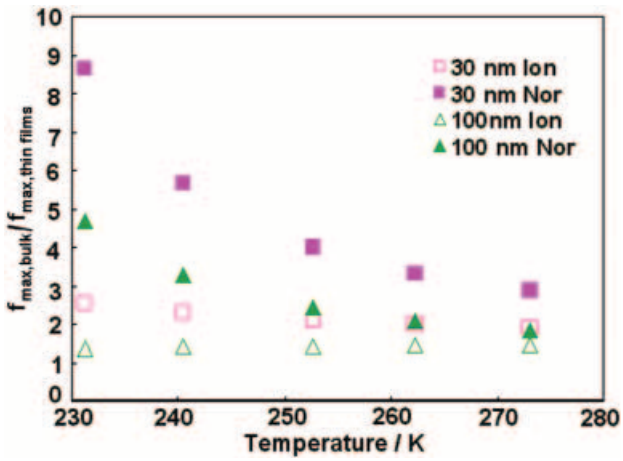

Fig. 5. The ratio of the bulk relaxation peaks, to those in the thin films, for the films of thickness 100 nm (triangles) and 30 nm (squares), plotted against absolute temperature. This ratio, shown for the normal-mode peak (filled symbols) and the ion peak (open symbols), was calculated from the Volger-Fulcher fits to the raw data, shown in Figure 4.

thickness, was also observed by us in a different system, *cis*-polyisoprene [16].

The thickness dependence of these modes is summarized in Figure 5, where the ratio of the peak relaxation frequency, in the bulk and in the thin films, is plotted against temperature. To make this calculation, the data in Figure 3 were fitted with the Volger-Fulcher curves drawn in Figure 3. It is evident that retardation began at higher temperatures, the thinner the film.

4 Discussion and outlook

There are several surprising aspects to these phenomenological findings. First, it is amazing to observe thickness-dependent relaxation modes for samples that were so thick relative to the molecular dimension. The end-to-end di-

mension of PPO can be estimated as $R_{\mathrm{ETE}} \approx 3$ nm —far less than the thickness, ≈ 100 nm, at which these effects were first observed.

Secondly, in mainstream theories of polymer dynamics there is supposed to be no difference between the temperature dependence of normal-mode and segmental relaxations; both are proportional to the monomeric friction coefficient [3]. The relaxation rate of the chain is separated into the product of the monomeric friction coefficient and geometrical factors that describe the chain itself, and the differences according to the degree of polymerization (N) depend on factors of N. The success of this interpretation is the basis of time-temperature superposition [3]. The data presented above can be interpreted as showing significant breakdown of time-temperature superposition in these thin films.

While there is some precedent for discrepancy when a bulk sample approaches T_{g} [32,33], for bulk samples those effects are observed only in much closer proximity to T_{g}, closer to T_{g} by an order of magnitude of temperature Kelvin [3,32,33]. We emphasize that all of these experiments concern temperature at least 30 K above the bulk T_{g}.

We have given much thought to possible mechanisms by which it might be possible to explain these findings trivially. First, concerns have often been expressed, regarding the case of much higher-molecular-weight chains than in the present study, that anomalous behavior related to the glass transition in thin polymer films might be introduced by orientation induced by spin-coating. In those samples it might not be possible to anneal spin-induced orientation completely, but this would not be reasonable to argue here. The anomalies reported here were largest for the samples of lowest molecular weight, whose relaxation time was the most rapid, and furthermore the sample preparation times far exceeded the longest relaxation times ($\approx 1/f_{\max}$), measured directly in these experiments. Therefore the chain configurations in these thin-film samples appear to have been equilibrated. Secondly, it is not reasonable to explain these findings by supposing that the sample became partitioned into two populations, one with the same properties as a bulk sample, and a second with surface-modified properties, as has been done for fluids confined within curved pores [34,35]; the thickness of a surface-bound layer, on the order of the end-to-end distance, was too much less than the total thickness. Therefore, the preponderant contribution to the measured responses should come from chains in the interior of the confined geometry. Third, it does not seem reasonable to dismiss these results as a trivial outcome of dewetting. While it is true that some small amount of dewetting was always present, metastable thin films could be produced, and reversibility of these measurements was confirmed (as discussed in Sect. 2).

Therefore, all things considered, we take these phenomenological measurements to be legitimate challenges for theoretical understanding. This study differs from most studies in this area in that the confinement was symmetric and without strong attraction to the walls. In this respect it resembles the study of free-standing films [36], but unlike that case the approach to study dielectric responses after confinement between dewetting solid surfaces makes it possible to study normal-mode responses significantly above the bulk glass transition temperature. Whether the rigidity of the walls might influence chain relaxation times owing to mechanical interaction with viscoelastic eigenmodes [37] is an interesting recent suggestion. Indeed, it remains an open question whether these confinement-induced effects have a fundamental relation to the glass transition problem, or perhaps stem for other reasons from geometrical confinement.

It is worth emphasizing that recently we measured qualitatively similar slowing down of the normal mode, but not the segmental mode, when *cis*-polyisoprene was confined between (dewetting) mica sheets [16]. To observe the same in this second system of flexible polymer chains suggests that the phenomenon is not system-specific.

We thank Prof. Hiroshi Watanabe in Kyoto University for discussion of this work. K.K. is also indebted to the Foundation of Kyushu Industrial Technology Center for financial support for the opportunity to perform this work. At the University of Illinois, this work was supported by the US Department of Energy, Division of Materials Science under Award Number DEFG02-91ER45439 to the Frederick Seitz Materials Research Laboratory at the University of Illinois at Urbana-Champaign.

References

1. G. Adam, J.H. Gibbs, J. Chem. Phys. **43**, 139 (1965).
2. M. Goldstein, J. Chem. Phys. **51**, 3728 (1969).
3. J.D. Ferry, *Viscoelastic Properties of Polymers*, 3rd edition (Wiley, New York, 1980).
4. M.T. Cicerone, F.R. Blackburn, M.D. Ediger, J. Chem. Phys. **102**, 471 (1995).
5. U. Tracht, M. Wilhelm, A. Heuer, H. Feng, K. Schmidt-Rohr, H.W. Spiess, Phys. Rev. Lett. **81**, 2727 (1998).
6. A. Onuki, R. Yamamoto, J. Non-Cryst. Solids **235**, 34 (1998).
7. C. Bennemann, C. Donati, J. Bashnagel, S.C. Glotzer, Nature **399**, 246 (1999).
8. C. Wang, M. Ediger, J. Chem. Phys. **112**, 6933 (2000).
9. E. Hempel, G. Hempel, A. Hensel, C. Schick, E. Donth, J. Phys. Chem. B **104**, 2460 (2000).
10. G. McKenna *et al.*, J. Non-Cryst. Solids **131**, 528 (1991).
11. J.L. Keddie, R.A.L. Jones, R.A. Cory, Europhys. Lett. **27**, 59 (1994).
12. For references to a large literature see D.S. Fryer, P.F. Nealey, J.J. de Pablo, Macromolecules **33**, 6439 (2000); S. Ge *et al.*, Phys. Rev. Lett. **85**, 2340 (2000); J. Park, G. McKenna, Phys. Rev. B **61**, 6667 (2000); J. Forrest, J. Mattsson, Phys. Rev. E **61**, R53 (2000); T. Kajiyama *et al.*, Macromolecules **30**, 280 (1997).
13. J. Forrest, K. Dalnoki-Veress, J. Dutcher, Phys. Rev. E **56**, 5705 (1997).
14. K. Dalnoki-Veress, J.A. Forrest, P.-G. de Gennes, J.R. Dutcher, J. Phys. IV **10**, 221 (2000).
15. Y.K. Cho, H. Watanabe, S. Granick, J. Chem. Phys. **110**, 9688 (1999).

16. S. Jeon, S. Granick, Macromolecules **34**, 8490 (2001).
17. J. McCallum, C. Vincent (Editors), *Polymer Electrolytes Review*, Vol. **1** (Elsevier, London, 1987) p. 173.
18. J.P. Donoso, T.J. Bonagamba, H.C. Panepucci, L.N. Oliveira, W. Gorecki, C. Berthier, M. Armand, J. Chem. Phys. **98**, 10026 (1993).
19. E. Tsuchida, N. Kobayashi, H. Ohno, Macromolecules **21**, 96 (1988).
20. T. Furukawa, M. Imura, H. Yuruzume, Jpn. J. Appl. Phys. **36**, 1119 (1997).
21. M. McLin, A. Angell, Polymer **37**, 4713 (1996).
22. T. Furukawa, K. Yoneya, Y. Takahashi, K. Ito, H. Ohno, Electrochim. Acta **45**, 1443 (2000).
23. M. Watanabe, J. Ikeda, I. Shinohara, Polym. J. **15**, 65 (1983).
24. G. Mao, R. Perea, W. Howells, D. Price, M. Saboungi, Nature **405**, 163 (2000).
25. S. Inoue, Y. Kimura, K. Ito, R. Hayakawa, Jpn. J. Appl. Phys. **38**, L665 (1999).
26. M. Baur, W. Stockmayer, J. Chem. Phys. **43**, 4319 (1965).
27. E. Niclo, T. Nicolai, D. Durand, Macromolecules **32**, 7530 (1999).
28. J. Schuller, Y. Mel'nichenko, R. Richert, E. Fischer, Phys. Rev. Lett. **73**, 2224 (1994)
29. R. Pelster, Phys. Rev. B **59**, 9214 (1999).
30. J. Korb, L. Malier, F. Cros, S. Xu, J. Jonas, Phys. Rev. Lett. **77**, 2312 (1996)
31. K.A. Barnes, A. Karim, J.F. Douglas, A.I. Nakatani, H. Gruel, E.J. Amis, Macromolecules **33**, 4177 (2000).
32. A. Schonhals, Macromolecules **26**, 1309 (1993).
33. D. Plazek *et al.*, J. Chem. Phys. **98**, 6488 (1993).
34. D. Boese, F. Kremer, Macromolecules, **23**, 829 (1990).
35. A. Rizos, G. Fytas, A. Semenov, J. Chem. Phys. **102**, 6931 (1995).
36. J. Forrest, K. Dalnoki-Veress, J. Dutcher, Phys. Rev. E **56**, 5705 (1997).
37. S. Herminghaus, K. Jacobs, R. Seemann, Eur. Phys. J. E **5**, 531 (2001).